AIP | Review of Scientific Instruments

Development of scanning x-ray fluorescence microscope with spatial resolution of 30 nm using Kirkpatrick-Baez mirror optics

S. Matsuyama, H. Mimura, H. Yumoto, Y. Sano, K. Yamamura, M. Yabashi, Y. Nishino, K. Tamasaku, T. Ishikawa, and K. Yamauchi

Citation: Review of Scientific Instruments **77**, 103102 (2006); doi: 10.1063/1.2358699
View online: http://dx.doi.org/10.1063/1.2358699
View Table of Contents: http://scitation.aip.org/content/aip/journal/rsi/77/10?ver=pdfcov
Published by the AIP Publishing

Development of scanning x-ray fluorescence microscope with spatial resolution of 30 nm using Kirkpatrick-Baez mirror optics

S. Matsuyama, H. Mimura, H. Yumoto, and Y. Sano
Department of Precision Science and Technology, Graduate School of Engineering, Osaka University, 2-1 Yamada-oka, Suita, Osaka 565-0871, Japan

K. Yamamura
Research Center for Ultra-Precision Science and Technology, Graduate School of Engineering, Osaka University, 2-1 Yamada-oka, Suita, Osaka 565-0871, Japan

M. Yabashi
SPring-8/Japan Synchrotron Radiation Research Institute (JASRI), 1-1-1 Kouto, Sayoucho, Sayogun, Hyogo 679-5148, Japan

Y. Nishino, K. Tamasaku, and T. Ishikawa
SPring-8/RIKEN, 1-1-1 Kouto, Sayoucho, Sayogun, Hyogo 679-5148, Japan

K. Yamauchi
Department of Precision Science and Technology, Graduate School of Engineering, Osaka University, 2-1 Yamada-oka, Suita, Osaka 565-0871, Japan

(Received 21 July 2006; accepted 27 August 2006; published online 11 October 2006)

We developed a high-spatial-resolution scanning x-ray fluorescence microscope (SXFM) using Kirkpatrick-Baez mirrors. As a result of two-dimensional focusing tests at BL29XUL of SPring-8, the full width at half maximum of the focused beam was achieved to be 50×30 nm^2 ($V\times H$) under the best focusing conditions. The measured beam profiles were in good agreement with simulated results. Moreover, beam size was controllable within the wide range of 30–1400 nm by changing the virtual source size, although photon flux and size were in a trade-off relationship. To demonstrate SXFM performance, a fine test chart fabricated using focused ion beam system was observed to determine the best spatial resolution. The element distribution inside a logo mark of SPring-8 in the test chart, which has a minimum linewidth of approximately 50–60 nm, was visualized with a spatial resolution better than 30 nm using the smallest focused x-ray beam. © *2006 American Institute of Physics.* [DOI: 10.1063/1.2358699]

I. INTRODUCTION

In the hard x-ray region, x rays having beam sizes of less than 100 nm have already been realized using optical devices such as Fresnel zone plates,[1] refractive x-ray lenses,[2] and Kirkpatrick and Baez (KB) mirrors.[3–7] Hard x-ray microscopes equipped with these focusing devices are currently hot topics of research and development. Actually, the applications of x-ray microscopes have expanded to various fields of material,[8] medical and biological sciences.[9–11]

A scanning x-ray fluorescence microscope (SXFM) is an imaging tool with which the element distribution of a sample can be visualized using x-ray fluorescence generated by the focused hard x-ray irradiation of the sample. Because the excitation beam consists of hard x rays, there is no need to install samples under vacuum.

In this microscopy, spatial resolution and sensitivity depend on, respectively, beam size and photon flux. From the viewpoint of sensitivity, the combination of a synchrotron radiation source, which can generate the brightest x ray, and KB mirrors, which have high focusing efficiency, is one of the most powerful focusing systems for a SXFM. In terms of spatial resolution, the previous report[4] regarding hard x-ray nanofocusing suggests that KB mirrors enable us to obtain a nanobeam having a full width at half maximum (FWHM) of better than 40 nm. Owing to achromatic focusing using total reflection on a mirror surface, we can select the most efficient energy of x rays for various samples and experimental conditions.

In this study, we developed a SXFM which makes it possible to visualize the element distribution inside a sample at a high spatial resolution better than 30 nm using both KB mirrors focusing system and an energy-dispersive spectrometer as an x-ray fluorescence detector. The most important feature is that the mirrors employed in this study were optimally designed and fabricated to achieve diffraction-limited focusing at 45 m downstream of a virtual light source produced by a slit. Owing to the distance of 45 m, x-ray beam size is controllable over a wide range by merely adjusting a virtual light source size.

Focusing tests and demonstration of the SXFM were performed at the new second experimental hutch (EH2) of BL29XUL[12] (SPring-8). As a result of focusing tests, a beam size of 30×50 nm^2 was achieved under the diffraction-limited condition by selecting a light source size of less than 10 μm. Moreover, beam size could be controlled over a wide range from 30 to 1400 nm (at FWHM) by changing light

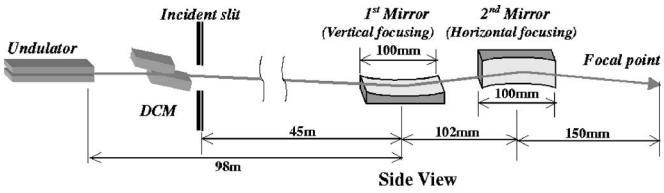

FIG. 1. Optical system designed for hard x-ray nanofocusing.

source size from 10 to 1000 μm. These results are in good agreement with simulated beam profiles. It was confirmed that the focusing system has good controllability for the SXFM. As a result of observation of a SPring-8 logo mark having a size of approximately 3×0.7 μm^2 on a test chart, the SXFM enabled us to visualize the element distribution of the logo mark at a spatial resolution better than 30 nm.

II. SCANNING X-RAY FLUORESCENCE MICROSCOPE

A. X-ray focusing optical system using KB mirrors

The new EH2 at BL29XUL of SPring-8 was newly built in May 2005 to study hard x-ray nanofocusing and hard x-ray microscopy. This hutch is placed 98 m downstream of an undulator. To utilize this hutch as efficiently as possible, KB mirrors designed specially for the hutch were fabricated with a figure accuracy of subnanometer order in Osaka University.[13–15] Available x-ray energy was selected to be less than 19 keV to be able to detect all elements using x-ray fluorescence (available within the range of 4.4–19 keV at BL29XUL). Working distance was designed to be relatively long (as long as 100 mm) considering the practical use of the x-ray microscope system, so that we keep the room where users can apply x-ray nanobeams in various experiments by only replacing a sample-scanning unit just downstream of the focusing system. A TC1 slit[16] located just downstream of a double-crystal monochromator (DCM) is used to control virtual light source size. The optical system and parameters of elliptical mirrors employed in the SXFM system are shown in Fig. 1 and Table I.

In the case of a relatively short distance of 45 m from a virtual light source to mirrors, the lower limit of beam size does not depend on only mirror aperture and focal length but also largely on light source size. However, under the condition of an adequately small source size, the smallest focus size is limited by mirror aperture size and focal length, i.e., the diffraction limit. In this case, photon flux and beam size are in a trade-off relationship. Figure 2 shows relationships between TC1 slit size and beam size predicted by wave-optical calculations. Under the conditions of a slit size of smaller than 10 μm, it is expected that diffraction-limited focusing can be realized. The slit can be no longer opened beyond a size of 1 mm because the beam broadening at the position of the slit is approximately 900×600 μm^2 (FWHM, $H\times V$). As a result of this calculation, it was expected that the beam size could be easily controlled within the range from 29 nm to micron order merely by changing the slit size from 10 to 1000 μm.

TABLE I. Parameters of elliptical mirrors.

	First mirror	Second mirror
Glancing angle (mrad)[a]	3.80	3.60
Mirror length (mm)	100	100
Mirror aperture (μm)	382	365
Focal length (mm)	252	150
Numerical aperture	0.75×10^{-3}	1.20×10^{-3}
Coefficient a of elliptic function (mm)	23.876×10^{3}	23.825×10^{3}
Coefficient b of elliptic function (mm)	13.147	9.609
Diffraction limited focal size (nm, FWHM)	48	29

[a]Glancing angle at the center of the mirror.

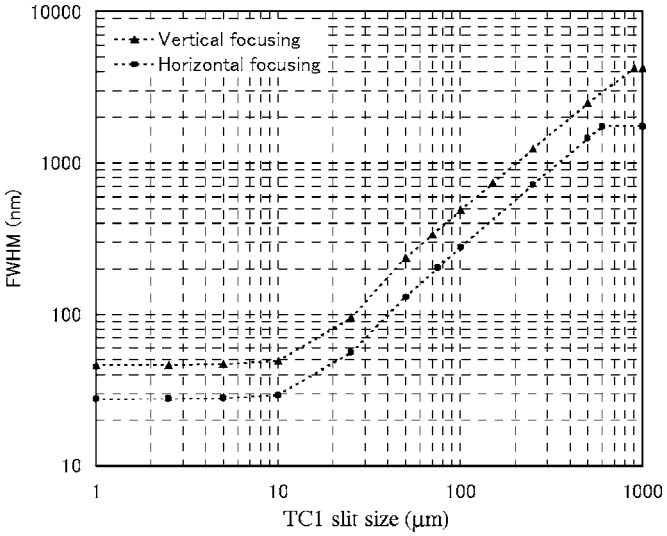

FIG. 2. Relationship between slit size and FWHMs predicated by wave-optical calculation.

B. SXFM system

Figure 3 shows a schematic drawing of the SXFM system. A mirror manipulator,[17] which was developed specially for high-accuracy positioning of KB mirrors, enables adjustment of mirror angle with the alignment accuracy required for diffraction-limited focusing. To detect x-ray fluorescence and transmitted x rays, respectively, a silicon drift detector (SDD, Röntec, Co., Ltd.) and a *p-i-n* photodiode were em-

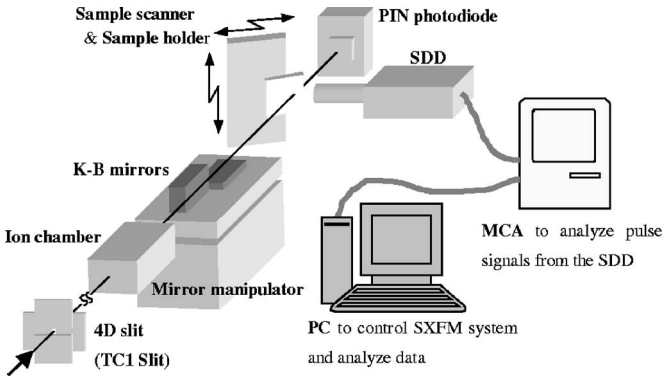

FIG. 3. Schematic drawing of scanning x-ray fluorescence microscope system.

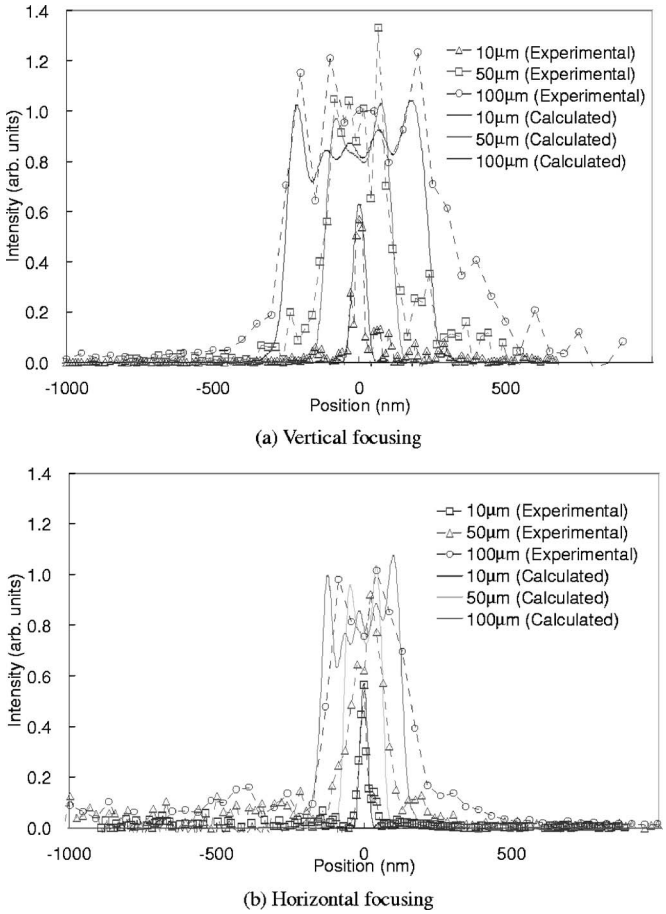

FIG. 4. Focused beam profiles obtained with KB mirrors. Subscripts at the top right show virtual source size.

ployed. An ion chamber just upstream of the mirrors is placed to normalize output data obtained with the SDD and *p-i-n* photodiode. A sample and a linear-encoder-based feedback *X-Y* stage having a positioning resolution of 1 nm (Sigma Tech, Co., Ltd.) are inclined at a 60° angle to the incident x-ray beam to set up the SDD near the sample. A cross wire is mounted on the *X-Y* stage near the sample to measure the intensity profiles at the focal plane by a wire scanning method with a gold wire of 200 μm in diameter.

III. FOCUSING TEST

Focusing tests were performed at the EH2 of BL29XUL at an x-ray energy of 15 keV. After finely tuning mirror positional alignments, beam profiles were measured by a wire scanning method, changing the virtual light source size. Experimentally obtained profiles and wave-optically simulated[18] ones are drawn, respectively, with dots and solid lines in Fig. 4. As a result of focusing tests, we could achieve two-dimensional diffraction-limited focusing having a FWHM of 30×50 nm^2 under the condition of a TC1 slit size less than 10 μm. Moreover, it was confirmed that beam size was controllable within the range of 30–1400 nm (at FWHM) by changing the slit size of a virtual source, although beam size and photon flux were in a trade-off relationship. To estimate the photon flux of focused beams, the number of x-ray photons collected by mirrors was calculated using the value counted by the *p-i-n* photodiode. The relationship between measured photon flux and estimated beam size is summarized in Table II. As can be seen from the table, the focused beams having a photon flux from 8×10^{12} photons/s (beam size: 1400×1000 nm^2) to 6×10^{9} photons/s (beam size: 30×50 nm^2) were available in the optical system.

TABLE II. Relationship between estimated beam size and measured photon fluxes.

Virtual source size $(H\times V)$ (μm^2)	Beam size $(H\times V)$ (nm^2)	Photon flux (photons/s)
10×10	29×48[a]	6×10^{9}
50×50	131×232	3×10^{11}
200×200	571×984	4×10^{12}
1000×1000 (Fully open)	$\sim1400\times\sim1000$	8×10^{12}

[a]Diffraction limit.

IV. PERFORMANCE TEST FOR SXFM SYSTEM

A. Evaluation of spatial resolution

A fine test chart was observed to evaluate the zoom function and the best spatial resolution of the SXFM. The test chart (shown in Fig. 5) was microfabricated on a Si_3N_4 substrate (200 nm thickness, NTT-AT, Co., Ltd.) using a focused ion beam (FIB) system (Hitachi, Co., Ltd., FB-2100). Figure 5 shows an image of secondary electrons emitted by FIB. White and black areas correspond to tungsten (W) deposition and the substrate, respectively. In this case, the smallest logo mark has 50–60 nm linewidths.

We observed the pattern using the SXFM, gradually being magnified with the beam having a size from 500 to 30 nm. Figures 6(1)–(4) show gallium (Ga) and W distribution maps visualized using the SXFM. Map (2) corresponds to the magnified image of the area marked by a white line in map (1), and maps (3) and (4) correspond to a logo mark of SPring-8 enclosed by the dashed square in map (2). Additionally, maps (5) and (6), which were visualized at a scanning pitch of 15 nm, are magnified images of only characters in map (3) and (4). Graphs in maps (5) and (6), which are line profiles along the dashed line in the W and Ga distribution maps, are plotted with a step of 15 nm. Table III shows the scan parameters of the SXFM observations. In this test chart, gallium remains in the regions where the ion beam was irradiated because liquid gallium was employed as an

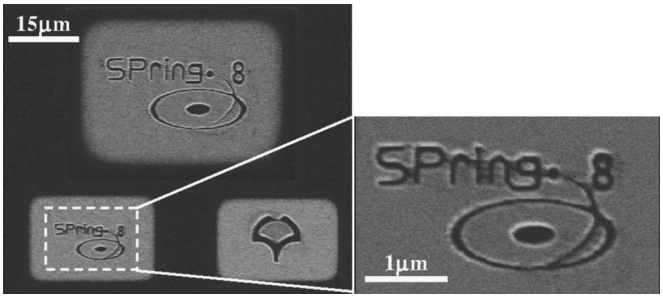

FIG. 5. Test pattern fabricated using FIB system.

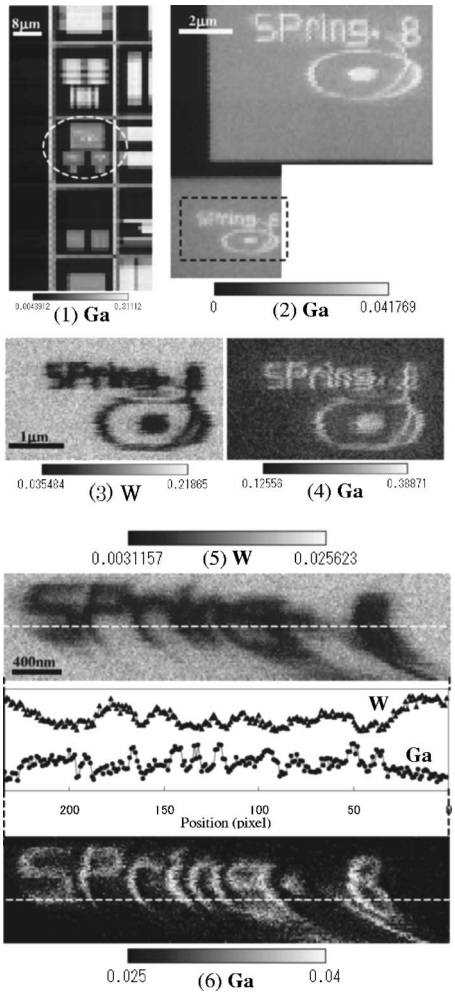

FIG. 6. Observation results of test chart using SXFM. Scan parameters are shown in Table III. Graphs of (5) and (6) show line profiles along the dash line in the W and Ga distribution maps.

ion source. As can be seen from the line profile in (6), it is found that the Ga distribution image acquired with the step of 15 nm/pixel could be visualized at a spatial resolution of 2 pixels, corresponding to 30 nm. Unlike the sharp pattern in the Ga distribution map, we cannot see sharp edges of the characters in the W distribution map in (5) because sidewall of characters patterned on the W deposition has a tapered shape. In contrast to the good results, the artifacts such as stripes and distortions are seen in Figs. 6(3)–6(6). They seem to be caused by thermal drifts of the sample, the sample scanning system, and the optical system. In this experience, the thermal stability of the whole SXFM system was within ±0.1 °C.

TABLE III. Scan parameters of SXFM. Exposure time: 1 s/pixel for each scan.

Map No.	TC1 Slit size ($V\times H$) (μm^2)	Scanning pitch (nm/pixel)	Scan area ($V\times H$) (μm^2)
(1)	150×90	1000	80×40
(2)	30×18	100	9.7×9.3
(3), (4)	10×10	30	2.25×4.02
(5), (6)	10×10	15	0.84×3.51

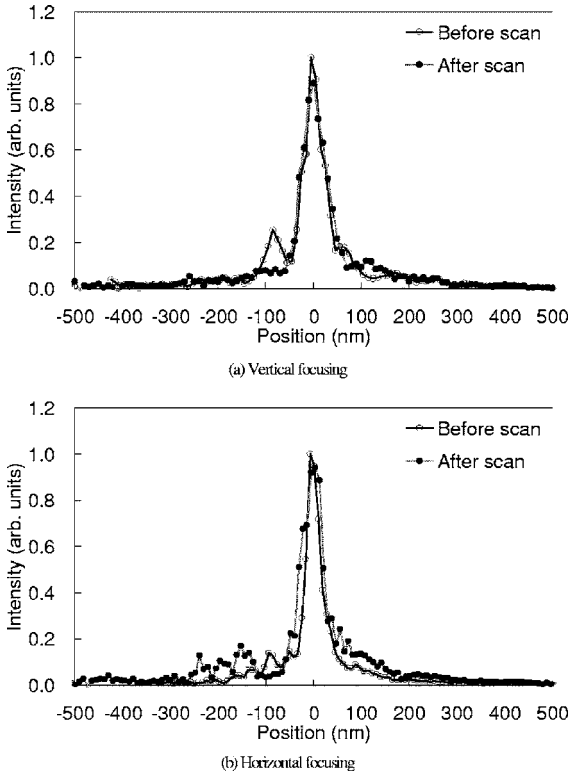

FIG. 7. Beam profiles before and after long scanning shown in Figs. 6(5) and 6(6). The time difference between the profiles is 8 h.

B. Stability of focused x-ray beam

The time required to acquire an image using a scanning x-ray microscope is 1–10 h generally, so it is important to keep the nanobeam stable during long periods of scanning. The stability of the nanobeam was evaluated by comparing beam profiles before and after high-resolution observation, as shown in Fig. 6(5) and (6) under the same condition. It took approximately 8 h to prepare the observation of the logo mark and acquire the high-resolution map. Figure 7 shows beam profiles before and after the observation. As a result of measurements of beam profiles, it was found that FWHM in horizontal focusing was broadened from 34 to 55 nm (where the beam profiles were measured at a 60° angle to the optical axis.). However, there was no change in FWHM in the vertical direction. We show results of measurements of temperature on the mirror manipulator and

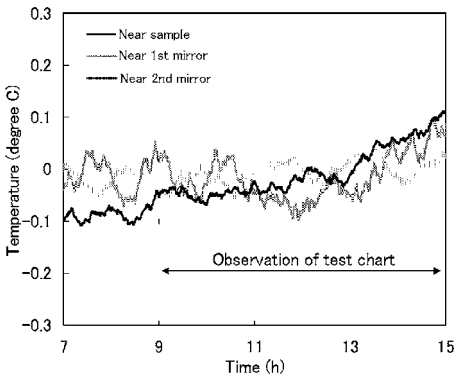

FIG. 8. Thermal stability of mirror manipulator and sample holder.

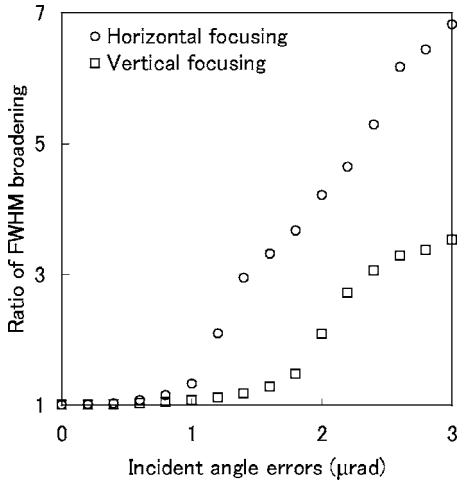

FIG. 9. Relationship between FWHM broadening and incident angle errors of the mirror. The vertical axis indicates the ratio to the best FWHM.

sample holder using thermocouples (type K) in Fig. 8. Owing to the absence of active thermal control over the whole SXFM system to avoid the vibration of the optical system, the temperature of the whole SXFM system gradually increased by 0.1–0.2 °C in 8 h. If the incident angles of two mirrors changed from the best angle to have a 1.2 μrad error in 8 h, the beam broadening caused by the misalignment is consistent with the wave-optically calculated results, showing the relationship between beam broadening and incident angle errors (shown in Fig. 9).

ACKNOWLEDGMENTS

This research was supported by Grant-in-Aid for Specially Promoted Research 18002009, 2006 and 21st Century COE Research, Center for Atomistic Fabrication Technology, 2006 from the Ministry of Education, Sports, Culture, Science, and Technology, Japan.

[1] Y. Suzuki, A. Takeuchi, H. Takano, and H. Talenala, Jpn. J. Appl. Phys., Part 1 **44**, 1994 (2005).
[2] C. G. Schroer *et al.*, Appl. Phys. Lett. **87**, 124103 (2005).
[3] P. Kirkpatrick and A. V. Baez, J. Opt. Soc. Am. **38**, 766 (1948).
[4] G. E. Ice, J.-S. Chung, J. Z. Tischler, A. Lunt, and L. Assoufid, Rev. Sci. Instrum. **71**, 2635 (2000).
[5] O. Hignette, P. Cloetens, W.-K. Lee, W. Ludwig, and G. Rostaing, J. Phys. IV **104**, 231 (2003).
[6] K. Yamauchi *et al.*, Jpn. J. Appl. Phys., Part 1 **42**, 7129 (2003).
[7] H. Mimura *et al.*, Jpn. J. Appl. Phys., Part 2 **44**, L539 (2005).
[8] T. Buonassisi, A. A. Istratov, M. A. Marcus, B. Lai, Z. Cai, S. M. Heald, and E. R. Weber, Nat. Mater. **4**, 676 (2005).
[9] K. M. Kemner *et al.*, Science **22**, 686 (2004).
[10] P. Ilinski *et al.*, Cancer Res. **63**, 1776 (2003).
[11] M. Shimura *et al.*, Cancer Res. **65**, 4998 (2005).
[12] K. Tamasaku, Y. Tanaka, M. Yabashi, H. Yamazaki, N. Kawamura, M. Suzuki, and T. Ishikawa, Nucl. Instrum. Methods Phys. Res. A **467**, 686 (2001).
[13] K. Yamauchi *et al.*, J. Synchrotron Radiat. **9**, 313 (2002).
[14] K. Yamauchi *et al.*, Rev. Sci. Instrum. **74**, 2894 (2003).
[15] H. Mimura *et al.*, Rev. Sci. Instrum. **76**, 045102 (2005).
[16] S. Goto, T. Hirono, and M. Tanaka, *MEDSI2004 Proceeding, Grenoble, France, 24–27 May 2004* (ESRF, Grenoble, 2004), p. 04-01.
[17] S. Matsuyama *et al.*, Rev. Sci. Instrum. (in press).
[18] K. Yamauchi *et al.*, Proc. SPIE **4782**, 271 (2002).